RESISTIVE DRIFT WAVES IN STELLARATORS

Ralf Kleiber

Max-Planck-Institut für Plasmaphysik, Teilinstitut Greifswald,
IPP-EURATOM-Association, Walther-Rathenau-Str. 49a, 17489 Greifswald

1. Introduction

Resistive drift waves are one possible mechanism for anomalous transport in the boundary region of fusion devices. Much work has been done on drift waves in tokamaks and their non-linear development into the turbulent regime can now be simulated.

Owing to their complicated structure the situation is totally different for stellarators: Even simple models of drift waves are not well understood.

In [1][2][3] the structure of linear non-resistive drift waves in stellarators was investigated. Instabilities caused by resistivity or trapped particles were considered in [4][5]. All these works make use of the ballooning formalism to reduce the drift wave equation to an ordinary differential equation which for each magnetic surface is solved along a field line and together with appropriate boundary conditions gives the eigenvalues.

This approach assumes perturbations varying rapidly perpendicular to the magnetic field. It also does not give the radial structure of the eigenmode.

Solving the general problem is much more difficult but gives the full mode structure.

2. Model equations

In order to obtain a model for resistive drift waves one starts with the linearized two-fluid-equations and make the following assumptions: Perturbed quantities $\sim e^{-i\omega t}$, cold ions, isothermal electrons, neglect of temperature perturbation, charge neutrality, electrostatic perturbations ($\beta \ll 1, \vec{E} = -\nabla\Psi$), constant electron collision time τ_{e}, vanishing electron mass in the electron equation, low frequency $\omega \ll \omega_{\mathrm{c,e}}$ ($\omega_{\mathrm{c,e}}$: electron gyrofrequency) and $\tau_{\mathrm{e}}\,\omega_{\mathrm{c,e}} \gg 1$ which allows to neglect the influence of the perpendicular resistivity. Also is is assumed that in the equilibrium state the electric field and the velocity vanish. Additionally the perturbation of the parallel ion velocity is neglected which eliminates the sound waves and thus reduces the dispersion relation from third to second order.

After normalizing space, time and potential to minor radius a, sound crossing time $\tau_{\mathrm{c}} = a/c_{\mathrm{s}}$ ($c_{\mathrm{s}}^2 = T_{\mathrm{e}}/m_{\mathrm{i}}$) and T_{e}/e the following equations in general geometry can be derived for density and potential perturbations ($\tilde{n}, \tilde{\Psi}$) :

$$\omega\frac{\tilde{n}}{n} + i\mathcal{A}\left(\vec{v}_* + \vec{v}_{\mathrm{d}}\right)\nabla\tilde{\Psi} - \omega\frac{\mathcal{A}^2}{B^2}\nabla\nabla_\perp\tilde{\Psi} = 0 \qquad (1)$$

$$\omega\frac{\tilde{n}}{n}+i\mathcal{A}\left(\vec{v}_*+\vec{v}_{\rm d}\right)\nabla\tilde{\Psi}-\frac{i}{n}\vec{v}_{\rm d}\nabla\tilde{n}+i\mathcal{C}\nabla\nabla_{\|}\left(\tilde{\Psi}-\frac{\tilde{n}}{n}\right)=0, \tag{2}$$

with the diamagnetic velocity

$$\vec{v}_*=-\frac{T_{\rm e}}{enB^2}\vec{B}\times\nabla n$$

and

$$\vec{v}_{\rm d}=\frac{2}{B^3}\vec{B}\times\nabla|\vec{B}|+\frac{1}{B^2}\nabla\times\vec{B}.$$

which for a vacuum field reduces to the curvature drift velocity. The parameters

$$\mathcal{A}=\frac{\rho_{\rm s}}{a} \qquad (\rho_{\rm s}=\frac{c_{\rm s}}{\omega_{\rm c,i}}),$$

$$\mathcal{C}=\frac{m_{\rm i}}{m_{\rm e}}\frac{\tau_{\rm e}}{\tau_{\rm c}}$$

represent a measure for inertia length and resistivity. In the limit of low resistivity (high $\mathcal{C}$) equation (2) gives the constituting relation for Boltzmann electrons.

Together with boundary conditions equations (1),(2) pose an eigenvalue problem for ω. The inner boundary condition stems from the requirement of a regular solution at $s=0$ (s: flux label):

$$\tilde{\Psi}_{\rm m,n}(0)=0 \qquad m\neq 0$$

$$\frac{\partial}{\partial s}\tilde{\Psi}_{\rm 0,n}(0)=0$$

(the same condition applies for $\tilde{n}$) while at the outer boundary the perturbation is forced to vanish

$$\tilde{\Psi}_{\rm m,n}(s=1)=0.$$

After formulating equations (1),(2) in magnetic (Boozer) coordinates a Fourier-decomposition in the poloidal and toroidal angle-like variables (Θ,Φ) is used:

$$\tilde{\Psi}=e^{i(M_{\rm p}\Theta+N_{\rm p}\Phi)}\sum_{\rm m=-M}^{\rm M}\sum_{\rm n=-N}^{\rm N}\tilde{\Psi}_{\rm m,n}(s)\,e^{i(m\Theta+n\Phi)}.$$

The numerical treatment of rapidly varying modes with high mode number is facilitated by introducing a phasefactor transformation which allows to shift the Fourier window $[-M:M]\times[-N:N]$ to $(M_{\rm p},N_{\rm p})$.

In the flux label the equations are discretized by 2nd-order Finite-Differences.

The resulting generalized complex non-hermitian matrix eigenvalue problem is solved by an implicitely restarted Arnoldi method. Since the Arnoldi method calculates a fixed number of eigenvalues nearest to a given spectral shift the complex plane has to be scanned to find the eigenvalues of interest.

A typical eigenmode calculation uses 100 gridpoints in the s-range $[0.9:0.97]$ (the outer boundary is located at $s=0.97$) and 21 Fourier components.

3. Equilibrium configuration

The code was developed to handle general three-dimensional equilibria as they are given by e.g. VMEC. Owing to the formulation in magnetic coordinates it only uses three independent metric coefficients which reflect all possible changes of geometry.

In order to keep the computational effort initially small, a straight l=2-stellarator with five field periods (topological torus), aspect ratio $A = 10$ and rotational transform ι running in the range $0.38 \dots 0.42$ was investigated. The density profile is bell shaped and gives a density scalelength $L_\mathrm{n} = |\nabla n/n|^{-1}$ which decreases towards the outer boundary.

The helical symmetry of the straight stellarator is exploited by a transformation to the helical coordinate $\alpha = 2\Theta - 5\Phi$ which reduces the problem to a two-dimensional one. In the case considered here (l=2-stellarator) the equilibrium can be described with sufficient accuracy by the two lowest helical Fourier components of the equilibrium quantities.

The physical parameters were fixed by using values for a typical edge region:
$a = 0.4\,\mathrm{m}$, $n = 10^{-19}\,\mathrm{m}^{-3}$, $B = 3\,\mathrm{T}$ and $T_\mathrm{e} = 200\,\mathrm{eV}$ giving $\mathcal{A} = 10^{-3}$ and $\mathcal{C} = 4 \cdot 10^3$.

4. Results

For given $M_\mathrm{P}, N_\mathrm{P}$ (where $M_\mathrm{P} > 200$ was choosen) the growthrate ω_i of the most unstable mode was calculated (these always have $\omega_r < 0$ while the modes with $\omega_r > 0$ are damped). Variation of M_P for fixed N_P shows that the growthrate has a maximum if the position of the corresponding resonant surface $\iota(s_R) = -(N_P - 5h)(M_P + 2h)^{-1}$ (h denotes the helical Fourier number) is near the minimum of L_n which in Figure 1 happens for $M_\mathrm{P} = 245$ and 255. The modes are dominated by the $h = 0$ Fourier component and modified by small sideband contributions.

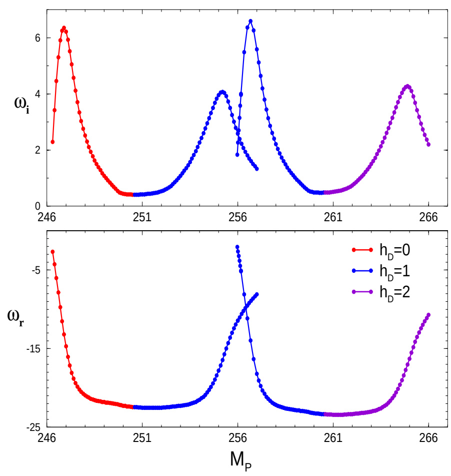

Figure 1. Imaginary and real part of ω as a function of M_P for $N_\mathrm{P} = -105$ for different modes. Colors indicate the dominant helical Fourier component h_D.

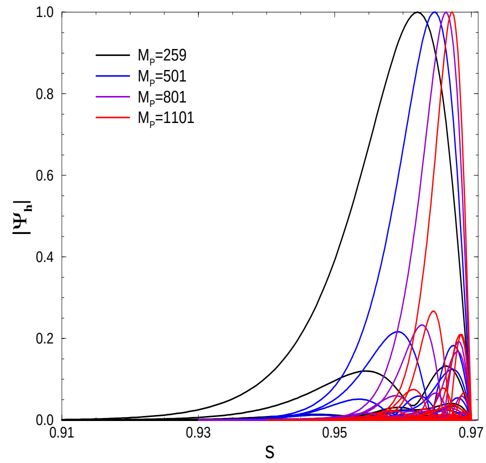

Figure 2. Modulus of the main Fourier components over flux label for the most unstable modes with M_P as shown and $N_P = -110, -213, -341, -469$.

They have no radial nodes and are located in a small region near the outer boundary (Figure 2). Modes with a higher radial node number start to become concentrated on both sides of the resonant surface but have a smaller growthrate than those with low node number (see Figure 3 where the resonant surface is resides at $s = 0.93$). If M_P is varied up to ≈ 2200 (Figure 4) the growthrate shows a maximum near $M_\mathrm{P} = 800$ ($\mathcal{A}\, M_P \approx 0.8$).

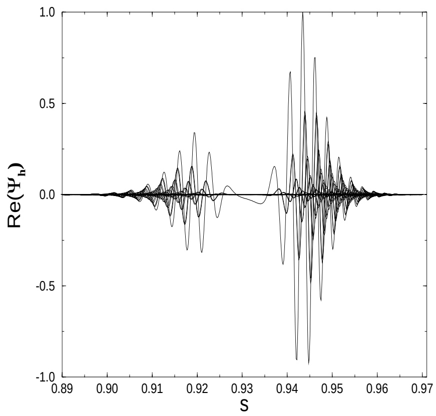

Figure 3. Real part of the main Fourier components for a mode with $M_\mathrm{P} = 259, N_\mathrm{P} = -110$ $(\omega_\mathrm{i} = -0.58 + 0.13i)$.

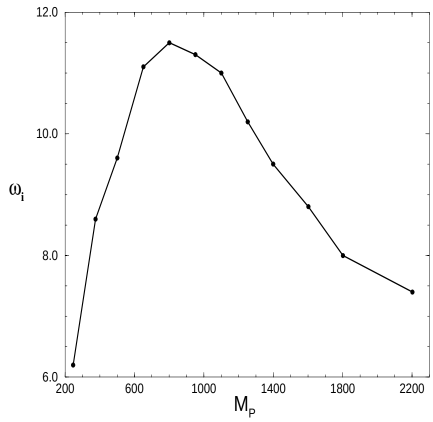

Figure 4. Growthrate of the most unstable mode (with $h = 0$ as dominant component) for given M_P and N_P.

5. Conclusion

For the first time eigenmodes of resistive drift waves in a straight l=2-stellarator were calculated without approximations regarding the equilibrium geometry or the mode structure. Since the developed code allows to investigate fully three-dimensional equilibria the topic of further study will be the influence of curvature and local shear on drift waves in toroidal stellarators. The code will also be applied to tokamak configurations in order to find possible structural differences in the drift mode structure.

Acknowledgements

I wish to thank J. Nührenberg for fruitful and encouraging discussions.

References

[1] A. Bhattacharjee et al.: Phys. Fluids **26**, 880 (1983)
[2] R.E. Waltz and A.H. Boozer: Phys. Fluids B **5**, 2201 (1993)
[3] M. Persson, J.L.V. Lewandowski, and H. Nordmann: Phys. Plasmas **3**, 3720 (1996)
[4] J.L.V. Lewandowski: Phys. Plasmas **4**, 4023 (1997)
[5] N. Dominguez et al.: Phys. Fluids B **4**, 2894 (1992)